4-1-2013

Synthesis and Polarographic Analysis of A2E

Elise Rivett
Olivet Nazarene University, erivett@olivet.edu

SYNTHESIS AND POLAROGRAPHIC ANALYSIS OF A2E

By

Elise Rivett

Honors Capstone Project

Submitted to the Faculty of

Olivet Nazarene University

for partial fulfillment of the requirements for

GRADUATION WITH UNIVERSITY HONORS

March, 2013

BACHELOR OF SCIENCE

in

Chemistry

WILLA HARPER	Willa Harper	3/18/13
Capstone Project Advisor (printed)	Signature	Date
CHARLES W. CRAIGHEAD		4/26/13
Honors Council Chair (printed)	Signature	Date
Janna R. McLean		4/10/13
Honors Council Member (printed)	Signature	Date

ACKNOWLEDGEMENTS

Thanks go to Dr. Larry Ferren for his assistance with polarography, to the Pence-Boyce scholarship committee of Olivet Nazarene University for financial support, to Dr. Elizabeth Gaillard of Northern Illinois University for the inspiration for this project, and to Dr. Jon Carnahan of Northern Illinois University for suggesting the DME. I would also like to thank Dr. Harper for editing my proposals, posters, and papers; for training me to use the rotary evaporator, gravity chromatography column, and HPLC; and for teaching me the fine art of creative problem-solving.

TABLE OF CONTENTS

LIST OF FIGURES

LIST OF TABLES

ABSTRACT

As humans age, fluorescent retinoid pigments accumulate in the retinal pigment epithelial (RPE) cells responsible for photoreceptor support. These fluorophores are of interest because they seem to contribute to diseases of the retina, particularly age-related macular degeneration, which is a leading cause of blindness in older adults in the United States and currently has no cure. One well-characterized fluorophore, A2E, can be oxidized by visible light and then generate harmful oxidative species capable of inducing programmed cell death in RPE cells. Further characterization of the redox behavior of A2E could ultimately aid the development of macular degeneration treatments designed to mitigate the harmful effects of oxidized A2E.

The purpose of this project was to estimate the reduction potential of A2E experimentally. A2E was synthesized by combining all-*trans*-retinal and ethanolamine in a 2:1 molar ratio, and separation was achieved by gravity chromatography followed by reverse phase HPLC. The presence of A2E was confirmed by measuring its absorbance spectrum. Linear sweep polarographic analyses of A2E were carried out using either tetrabutylammonium hexafluorophosphate (TBAHFP) or sodium chloride as the supporting electrolyte. Trials with TBAHFP solution produced one-wave polarograms, while trials with sodium chloride solution yielded two-wave polarograms. However, the polarograms obtained for A2E solutions were very similar to those produced by control solutions, indicating the need for procedural modifications.

Keywords: A2E, blindness, macular degeneration, N-retinylidene-N-retinylethanolamine, polarography, reduction potential, retinal pigment epithelium, vision loss

INTRODUCTION

As humans age, fluorescent retinoid pigments accumulate in the retinal pigment epithelial (RPE) cells responsible for photoreceptor support (Dorey et al., 1989; Feeney-Burns et al., 1984; Gaillard et al., 1995; Kennedy et al., 1995; Sarks et al., 1980; Sparrow et al., 1999). These fluorophores are of interest because high levels of these fluorophores are associated with several diseases of the retina, including early-onset macular degeneration (Stargardt's disease) and age-related macular degeneration (AMD) (Ben-Shabbat et al., 2002; Birnbach et al., 1994; Gaillard et al., 1995; Hogan, 1972; Lopez et al., 1990). Since AMD is a leading cause of blindness in older adults in the United States and currently has no cure, further study of the fluorescent pigments in the RPE is warranted.

One particularly well-characterized component of the fluorescent pigments in the RPE is N-retinylidene-N-retinylethanolamine, more commonly called A2E (Liu et al., 2000). A2E is the product of a series of reactions between two molecules of the vitamin A derivative all-*trans*-retinal and one ethanolamine molecule (Eldred and Lasky, 1993; Liu et al., 2000; Sakai et al., 1996). This bisretinoid is capable of absorbing light via photooxidation and then damaging its cellular environment by generating dangerous oxidative species (Gaillard et al., 1995; Ragauskaite et al., 2001; Sparrow et al., 2000, 2002, 2003). Given the potentially destructive nature of A2E, it would be useful to find a compound that would shorten the lifetime of photooxidized A2E by reacting with it via a benign oxidation-reduction (redox) reaction. The reduction potential of A2E, if it were known, would be of invaluable help in predicting what type of compounds A2E could

react with readily and rapidly. The purpose of this project was to investigate A2E via polarography (a specific type of voltammetry) with the ultimate goal of finding the $E_{½}$ value of A2E, which is directly related to the reduction potential (Sawyer et al., 1984). To achieve this goal, A2E was synthesized, purified by gravity column chromatography, and analyzed polarographically.

REVIEW OF LITERATURE

Structure and Function of the Retina

For humans and other vertebrates, vision starts in the retina, the layer of tissue that forms the posterior lining of the eyeball, opposite the pupil (Dowling, 1987; Kolb, 2003; Kolb et al., 2001; Rodieck, 1998). The anatomy of the human retina (Fig. 1) is somewhat counterintuitive in that the photoreceptor cells are farthest from the pupil, meaning that light must pass through two cell layers, the inner nuclear and ganglion cell layers, before reaching the cells which initiate the response to light (Dowling, 1987; Hattar et al., 2002; Kolb, 2003; Kolb et al., 2001; Kolb and Famiglietti, 1974). The information the photoreceptors detect is relayed first to the nerve cells of the inner nuclear layer, then to the ganglion cells on the surface of the retina (Dowling, 1987; Hattar et al., 2002; Kolb 2003; Kolb et al., 2001; Kolb and Famiglietti, 1974; Rodieck, 1998). The ganglion cells communicate with nerve fibers that converge near the center of the eye to form the optic nerve, which carries visual information to the brain, where nerve signals are interpreted as images (Dowling, 1987; Kolb, 2003; Kolb et al., 2001; Kolb and Famiglietti, 1974; Rodieck, 1998).

GRAPHIC REDACTED

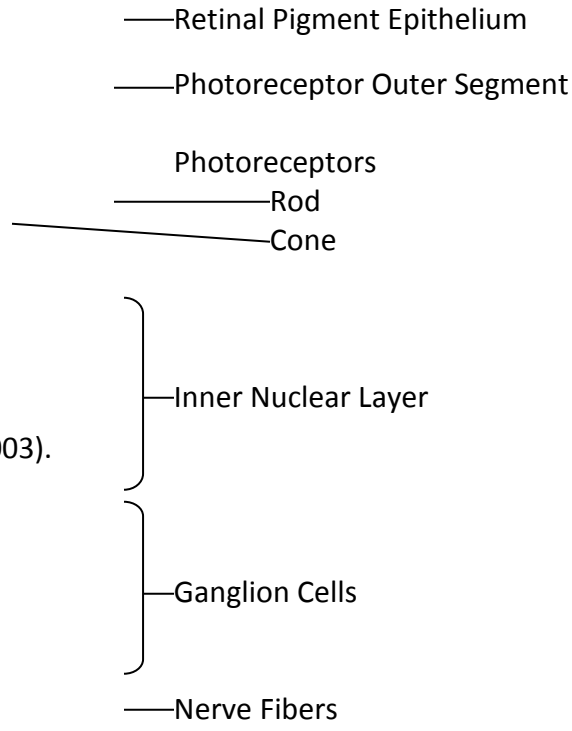

Figure 1. The layers of the retina (from Kolb, 2003).

There are two types of photoreceptors: rods and cones (Fig. 1). Cones function best under bright light conditions, and they allow for color perception. Rods cannot detect color, but they are sensitive to tiny amounts of light, enabling us to see under low light conditions. Rods and cones both contain a region known as the outer segment (Fig. 1) that is structurally distinct from the cell body; it is here that photons are detected. The outer segment is essentially a stack of disks made by infoldings of the plasma membrane. The membrane that forms the periphery of each disk contains the important transmembrane protein complex rhodopsin (Fig. 2; Dowling, 1987; Hattar et al., 2002; Kolb, 2003; Kolb et al., 2001; Rodieck, 1998). Rhodopsin is a protein molecule composed of seven helices that span the entire membrane (Hargrave, 2001; Unger et al., 1997). In the middle of these helices, there is a pocket where 11-*cis*-retinal (vitamin A aldehyde) binds (Hargrave, 2001; Hargrave et al., 1993). When light strikes the photoreceptor, 11-*cis*-retinal changes shape to become all-*trans*-retinal via a process called photoisomerization. This conformational change to all-*trans*-retinal causes the rhodopsin protein in which it is embedded to undergo a conformational change as well (Baylor, 1996; Hargrave, 2001; Pugh and Lamb, 1993; Yau, 1994). Rhodopsin's shape change initiates a series of chemical reactions known as the visual cascade that ultimately modifies the photoreceptor's communication with a nerve cell in the inner nuclear layer. In darkness, the photoreceptor continuously releases glutamate which is received by cells in the inner nuclear layer. When light reaches a photoreceptor, the photoreceptor stops glutamate transmission as a way of signaling the inner nuclear layer and starting visual information on its way to the brain (Baylor, 1996; Dowling,

1987; Hattar et al., 2002; Hargrave, 2001; Kolb, 2003; Kolb et al., 2001; Pugh and Lamb, 1993; Rodieck, 1998; Yau, 1994).

GRAPHIC REDACTED

Figure 2. The rhodopsin complex…
The rhodopsin complex is composed of the transmembrane protein opsin bound to 11-*cis*-retinal. Rhodopsin is found in the disk membranes of photoreceptor outer segments. (from Fisiologiauhu, 2013).

The Retinoid Cycle

Just posterior to the photoreceptors lies a layer of non-nerve cells known as the retinal pigment epithelium (RPE) (Dowling, 1987; Kolb, 2003; Kolb et al., 2001; Rodieck, 1998). The RPE supports the photoreceptors in a variety of ways. For the purpose of this discussion, the two most important roles of the RPE are phagocytosizing the outer segment fragments that photoreceptors continually shed and regenerating 11-*cis*-retinal from all-*trans*-retinal (Ben-Shabbat et al., 2001; Crouch et al., 1996).

As discussed above, the presence of 11-*cis*-retinal in the outer segments enables the photoreceptors to detect light. The all-important 11-*cis*-retinal molecules are transported to the photoreceptors from the RPE (Crouch et al., 1996). Although both rods and cones contain 11-*cis*-retinal, retinal metabolism may differ in rods and cones; less is currently known about the cones' pigment and cascade (Baehr and Liebaman, 2002; Crouch et al., 1996). The following paragraphs discuss retinoid transport and metabolism in rods.

RPE cells convert vitamin A (all-*trans*-retinol; Fig. 3) from the alcohol form to 11-*cis*-retinal (Fig. 4), the functional aldehyde form (Crouch et al., 1996). All-*trans*-retinol is a conjugated hydrocarbon chain attached to a hydrocarbon ring at one end and a hydroxyl group at the other end (Crouch et al., 1996). Once in the RPE, the structure of all-*trans*-retinol is modified in two ways: First, the bond at carbon 11 is converted to a *cis* bond via a two-step process, producing a bend in the hydrocarbon chain (Crouch et al., 1996; Rando, 1989, 1992). The hydroxyl group is then oxidized to a carbonyl group, yielding 11-*cis*-retinal (Crouch et al., 1996; Saari, 1994; Saari et al., 1994; Suzuki et al.,

1993). The newly made 11-*cis*-retinal can be transported to the photoreceptor outer segments (Crouch et al., 1996). In rod photoreceptors, the carbonyl group is converted to a protonated Schiff base in order to bind opsin and form the rhodopsin complex (Baehr and Liebman, 2002; Crouch et al., 1996; Sakmar et al., 1989; Wald, 1968; Zhukovsky and Oprian, 1989). At this point, 11-*cis*-retinal is ready to respond to light. As previously discussed, visible light changes 11-*cis*-retinal to all-*trans*-retinal (Fig. 5) and initiates the photoreceptor's signaling process (Baylor, 1996; Crouch et al., 1996; Hargrave, 2001; Pugh and Lamb, 1993; Yau, 1994).

After retinal has responded to light (a process called bleaching because it changes retinal from a colored product to a colorless one), inhibitory reactions return the cell to its pre-stimulus state (Crouch et al., 1996; Hofmann et al., 1992; Ishiguro et al., 1991). All-*trans*-retinol dehydrogenase then reduces all-*trans*-retinal to all-*trans*-retinol (vitamin A), causing it to dissociate from the rhodopsin complex (Crouch et al., 1996; Hofmann et al., 1992; Ishiguro et al., 1991). At this point, all-*trans*-retinol is ready to be sent back to the RPE to be converted to 11-*cis*-retinal and reused (Baehr and Liebman, 2002; Crouch et al., 1996).

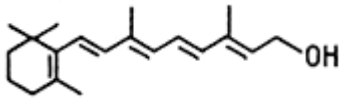

Figure 3. All-*trans*-retinol (Vitamin A). (Cyberlipids: Vitamin A, 2013).
RPE cells receive retinoids in the form of all-*trans*-retinol.

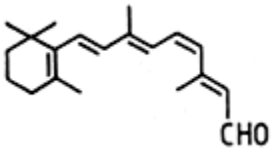

Figure 4. 11-*cis*-retinal. (Cyberlipids: Vitamin A, 2013).
11-*cis*-retinal is produced in the RPE and transported to the photoreceptors where it initiates rhodopsin's response to light.

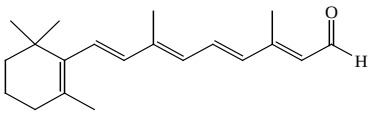

Figure 5. All-*trans*-retinal (Vitamin A aldehyde).
Photoisomerization converts 11-*cis*-retinal to all-*trans*-retinal in the photoreceptor. Normally, all-*trans*-retinal is reduced and returned to the RPE. However, it may also serve as a reactant in A2E biosynthesis.

Biosynthesis of A2E

Problems can arise if the last reaction in the retinoid cycle (the reduction of all-*trans*-retinal) occurs more slowly than the bleaching of 11-*cis*-retinal (Crouch et al., 1996; Zimmerman, 1974). If all-*trans*-retinal accumulates faster than the all-*trans*-retinol dehydrogenase can reduce it, some of the excess retinal can undergo a different reaction that ultimately leads to the formation of A2E, a potentially dangerous molecule (Ben-Shabbat et al., 2001; Crouch et al., 1996; Eldred and Lasky, 1993; Sakai et al., 1996; Ren et al., 1997; Zimmerman, 1974).

The first step in A2E formation appears to be the reaction between all-*trans*-retinal and phosphatidylethanolamine (Fig. 6), a phospholipid present in the photoreceptor's outer membrane (Eldred and Lasky, 1993; Liu et al., 2000; Sakai et al., 1996; Ren et al., 1997). These two molecules join together by forming a Schiff base (Liu et al., 2000; Katz et al., 1996; Parish et al., 1998). A second all-*trans*-retinal molecule is incorporated through further reactions, producing the A2E precursor A2-PE (Fig. 7; Liu et al., 2000). A2-PE is then converted to A2E (Fig. 8) via a hydrolysis reaction that removes the lipid group (Liu et al., 2000). Research done by Ben-Shabbat et al. (2001) indicates that A2-PE is converted to A2E in the photoreceptor membrane by a phosphodiesterase enzyme. If A2E is produced in the photoreceptor, as their study suggests, it is assumed that A2E enters the RPE when retinal pigment epithelial cells phagocytose discarded bits of the photoreceptor's outer segment (Ben-Shabbat et al., 2001). Regardless of how A2E arrives, it is known that it ultimately accumulates in RPE lysosomes, where it poses a threat to cell viability.

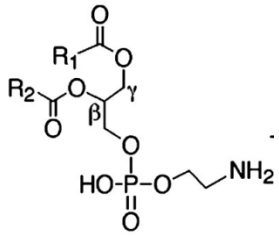

Figure 6. Phosphatidylethanolamine. (Liu et al., 2000).
The side chains R_1 and R_2 represent fatty acid chains with 14-22 carbons.

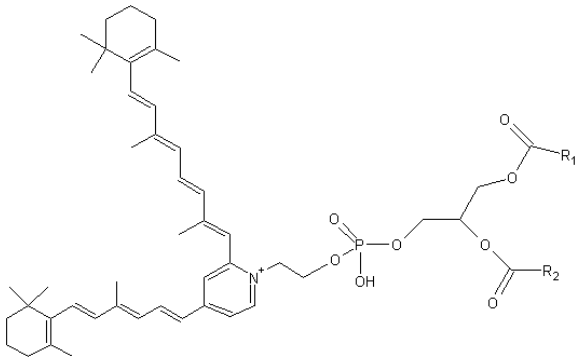

Figure 7. A2-PE (Phosphatidylethanolamine-bisretinoid)
(Cyberlipid Center: Ethanolamine glycerophospholipids, 2013). The side chains R_1 and R_2 represent fatty acid chains.

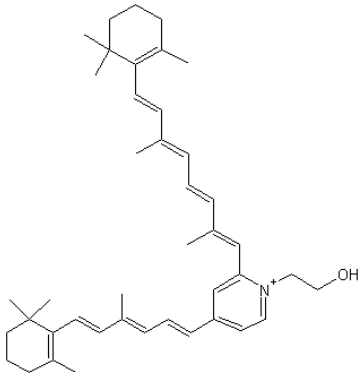

Figure 8. A2E (N-retinylidene-N-retinylethanolamine).
(Cyberlipid Center: Vitamin A, 2013).

A2E Characteristics and Potential Toxicity

A2E is a major component of the heterogeneous mixture of fluorophores that populate the lipofuscin granules in RPE cells. Lipofuscin accumulates in the RPE as humans age. The greatest increase in lipofuscin occurs between the ages of 10 and 20 years; the area of an RPE cell occupied by lipofuscin then remains fairly constant until the age of 50, at which point the percentage of cellular area taken up by lipofuscin begins to increase (Dorey et al., 1989; Feeney-Burns et al., 1984; Gaillard et al., 1995; Kennedy et al., 1995; Sarks et al., 1980; Sparrow et al., 1999).

Lipofuscin fluorophores do not merely serve as indicators of cellular age. High levels of these fluorophores are associated with several diseases of the retina, including early-onset macular degeneration (Stargardt's disease) and age-related macular degeneration (AMD), which can both lead to vision loss and blindness (Ben-Shabbat et al., 2002; Birnbach et al., 1994; Gaillard et al., 1995; Hogan, 1972; Lopez et al., 1990). In patients with these diseases, the borders of the atrophied portions of the retina exhibit increased levels of fluorescence, as do the regions that will be next to degenerate (Cideciyan et al., 2004; Einbock et al., 2005; Holz et al., 2001; Radu et al., 2005; Schmitz-Valckenberg, 2004; Spaide, 2003).

A2E is one of the most highly-characterized fluorophores of RPE lipofuscin. As a fluorophore, A2E absorbs visible light (Parish et al., 1998; Sparrow et. al, 2000). Its maximum absorbance is at 430 nm, in the blue light region (Parish et al., 1998; Sparrow et. al, 2000). A2E fluoresces by emitting lower-energy orange light; its maximum

fluorescence ranges from 510 nm to 615 nm, depending on the solvent (Ragauskaite et al., 2001).

The correlation between the presence of A2E and other fluorophores and retinal disease suggests that A2E is in some way toxic to its cellular surroundings. Early studies of human lipofuscin as a whole revealed that the mixture of fluorescent compounds could produce triplet and radical intermediates as well as singlet oxygen when photooxidized (Gaillard et al., 1995). Further studies showed that if A2E is photooxidized by light, especially blue light, it can generate myriad unstable, high energy species such as singlet oxygen, superoxide anions, hydrogen peroxide, and possibly even radicals (Boulton et al., 1993; Gaillard et al., 1995; Sparrow et al., 2000; Ragauskaite et al., 2001; Rozanowska et al., 1998; Wassel et al., 1999).

Several studies have been done to investigate the photooxidation products of A2E. Sparrow, Nakanishi, and Parish found that irradiating cultures of A2E-laden RPE cells with blue light significantly increased the number of apoptotic cells found in the culture, while cell cultures irradiated with green light remained normal (2000). The fact that blue light was significantly more harmful indicates that A2E, which absorbs blue light strongly, is involved in apoptosis, or cell-directed death (Sparrow et al., 2000). Another study, conducted by Sparrow et al., confirmed that cell viability decreased when A2E-laden cells were irradiated with blue light (2002). Interestingly, the addition of oxygen quenchers and scavengers protected cells from blue-light damage, indicating that singlet oxygen generated by A2E contributed to cell destruction (Sparrow et al., 2002). The photooxidation products of A2E also appear to activate inflammation-causing

complement proteins found in sub-RPE deposits of drusen (Zhou et al., 2006). Like lipofuscin, the accumulation of drusen is associated with AMD (Zhou et al., 2006). It is hypothesized that the purported role of A2E in complement activation could make the macula more susceptible to chronic inflammation and diseases such as macular degeneration (Zhou et al., 2006). Other studies have demonstrated that A2E, with its polar head and non-polar tails, can behave like a detergent, disrupting cell membranes. A2E also appears to be capable of generating singlet oxygen and then reacting with it to form A2E-epoxides. These A2E-epoxides may be responsible for the DNA lesions associated with blue-light damage observed in the RPE (Sparrow et al., 1999, 2003).

Clearly, A2E has the potential for damaging the retinal pigment epithelium in many ways, and most A2E-mediated mechanisms for cell injury involve photooxidized A2E oxidizing other species that harm the cell (Boulton et al., 1993; Gaillard et al., 1995; Ragauskaite et al., 2001; Rozanowska et al., 1998; Sparrow et al., 1999, 2000, 2002, 2003; Wassel et al., 1999; Zhou et al., 2006). Therefore, one method for mitigating the threat of A2E would be to find a species that reacts preferentially with A2E without generating a dangerous product. The reduction potential of A2E, if it were known, would be of invaluable help in predicting what type of compounds A2E could react with readily and rapidly. Reduction potentials are used to calculate whether a redox reaction between specific reactants is energetically favorable (Ebbing and Gammon, 2009). The goal of this research project was to investigate the reduction potential of A2E via polarography.

In Vitro Synthesis of A2E

Parish et al. (1998) developed a fairly straightforward one-pot method for synthesizing A2E that gives a 49% yield. Initial purification of the reaction mixture was achieved by using a gravity chromatography column packed with silica gel to separate unreacted all-*trans*-retinal from A2E based on hydrophobicity. They also reported an optimized method for isolating and identifying A2E in nanogram amounts using reverse phase HPLC. UV absorbance analysis was used to confirm the presence of A2E and *iso*-A2E. It was determined that A2E elutes slightly before *iso*-A2E, the most common photo-isomer of A2E. Through further studies of A2E and *iso*-A2E, it was also determined that upon exposure to light, A2E equilibrates with *iso*-A2E, giving a 4:1 A2E: *iso*-A2E ratio, which indicates that a sample of A2E must be kept in darkness to maintain its purity (Parish et al., 1998).

The one-pot synthesis method developed by Parish et al. (1998) has become a popular way to artificially synthesize A2E, no doubt due to the simplicity of the synthesis (Ben-Shabbat et al., 2002; Heo et al., 2012; Jee et al., 2012; Ragauskaite et al., 2001). The most significant drawback to this method is the amount of time required to purify A2E after synthesis (Jee et al., 2012). Silica gel chromatography and HPLC are both time-consuming processes, and a large scale preparation of A2E is also costly in terms of the amount of solvent that must be used for HPLC (Jee et al., 2012). Jee et al. (2012) have recently reported the successful use of a cation exchange resin as a more economical alternative to HPLC separation for scaled-up procedures. For the purpose of this study, a large-scale preparation was not needed. Therefore silica gel chromatography and HPLC

methods were used to separate A2E. As will be discussed below, the time-consuming nature of silica gel separation was evident even on a small scale.

Polarography

Polarography refers to the branch of voltammetry that uses a dropping mercury electrode (DME) as a working electrode (Skoog et al., 2007). In polarography, the voltage between the DME and the reference electrode is varied, and the resulting current that flows at the DME is measured (Sawyer et al., 1984). In a linear polarographic scan, the potential applied to the dropping mercury electrode is made increasingly negative throughout the scan. Eventually, the magnitude of the negative charge becomes great enough to initiate reduction of the analyte at the electrode surface. As soon as reduction begins, the amount of current flowing at the electrode increases dramatically (Sawyer et al., 1984). The mechanism is as follows: the mercury drop is surrounded by a small diffusion layer of solvent (Koryta, 1961). The ratio of oxidized and reduced species within this layer differs from the ratio in the rest of the solution (the bulk solution; Koryta, 1961; Zuman, 2006). Oxidized species diffuse to the electrode in response to this concentration difference, and the electrode measures this movement of ions as current (Sawyer et al., 1984; Zuman, 2006). As the magnitude of the voltage increases, the current also increases until the limiting diffusion current is reached (Sawyer et al., 1984; Zuman, 2006). The limiting diffusion current (i_d) is the current at which the reaction rate has reached its maximum. At this point, increasing the electrode's potential will not further increase the reaction rate or the current (Zuman, 2006).

Polarography was used to investigate the reduction potential of A2E because polarographic data can be used to calculate $E_{½}$ values. This value is defined as the potential at which the current equals ½ of the limiting diffusion current (i_d); this value is significant because it is directly related to the reduction potential of an analyte (Sawyer et al., 1984). Therefore, obtaining useful polarographic data could allow for the determination of the reduction potential of A2E.

Previously, our research group had synthesized A2E and studied it via cyclic voltammetry (CV; Taylor et al., 2008; White et al., 2006). Cyclic voltammetry and polarography are related methods: both measure the current induced at a working electrode in response to an applied potential (Sawyer et al., 1984). However, during CV scans, the potential is alternately decreased and then increased, allowing for the formation of both reduction and oxidation waves (Sawyer et al., 1984). Another key difference between CV and polarography is the composition of the working electrode: the working electrode in CV is a platinum wire, while a dropping mercury electrode (DME) is used in polarography (Skoog et al., 2007).

During the first set of CV analyses with A2E, a sample of A2E was used to determine that the best voltammograms are produced when A2E is dissolved in a very polar solvent, such as distilled water or a water/methanol mixture with a high percentage of water (Taylor et al., 2007). Sodium chloride was used as the supporting electrolyte during these initial trials (Taylor et al., 2007). In a separate experiment, CV analyses of A2E were run using tetrabutylammonium hexafluorophosphate (TBAHFP) as the supporting electrolyte (White et al., 2010). This method produced variable results

over time (White et al., 2010). The variation in results may have been caused by the products of side reactions, which can build up on the surface of the working electrode over time and affect the currents measured by the voltammeter (Skoog et al., 2007). It was to avoid this problem that a dropping mercury electrode (Fig. 9) was used in the present study. A DME is designed to allow mercury to flow through a thin capillary tube so that droplets continually form at the end of the tube and fall when they grow heavy (Skoog et al., 2007). Each droplet momentarily serves as the working electrode (Skoog et al., 2007). The advantage of a DME is that the working electrode surface is renewed each time a new drop of mercury forms, preventing extraneous materials from being deposited on the electrode and skewing current measurements (Skoog et al., 2007). The purpose of this study was to investigate the possibility of measuring the reduction potential of A2E by using a dropping mercury electrode and varying current linearly.

Figure 9. A dropping mercury electrode (from Bioanalytical Systems, Inc, 2012).

MATERIALS AND METHODS

A2E Synthesis

A2E synthesis, separation and HPLC analysis were carried out using a modified version of the procedure reported by the Parish group (Parish et al., 1998). New all-*trans*-retinal (purity ≥ 98%) was obtained from Sigma-Aldrich. Ethanolamine (purity 99+ %) was also purchased from Sigma-Aldrich. A2E was synthesized by combining all-*trans*-retinal and ethanolamine in a 2:1 molar ratio. Methanol obtained from VWR International was used as the solvent, and 10 µL of glacial acetic acid from Fisher Scientific was added to the reaction mixture. The mixture was allowed to stir for three days. Following synthesis, the mixture was dried with a rotary evaporator and stored in a -80˚ freezer. All work was carried out under low-light conditions.

Silica Gel Separation

The entire A2E synthesis mixture was loaded onto a gravity column for separation as shown in Figure 10. The column was packed with 200-400 mesh silica gel from Sigma-Aldrich. The sample was first eluted with 5:95 methanol:dichloromethane (CH_3OH:CH_2Cl_2), then with 8:92:0.002 CH_3OH:CH_2Cl_2:TFA (trifluoroacetic acid). The first solvent, which was less polar, was used to elute unreacted all-*trans*-retinal and other impurities. Four separate orange-brown bands were eluted and collected with the 5:95 solvent. Three more bands, labeled polar band 1, 2, and 3, respectively, were collected after the change to the more polar (8:92:0.002) solvent. Polar bands 2 and 3 were fairly dark in color and were dried with a rotary evaporator immediately after collection.

Figure 10. A silica gel chromatography column.
Two distinct bands (dark orange and yellow orange) are visible at the top of the column.

HPLC Separation

Polar bands 2 and 3 were examined on a Hitachi Elite LaChrom HPLC equipped with an L-2130 pump, an L-2450 diode array detector, and a 3.9 X 150 mm Waters Nova-Pak C18 Column. Two 20 µL samples were run for each band. Each run was 40 minutes long. For the first 10 minutes, the column was eluted with 75% methanol: 25% water (0.1% TFA). From 10 minutes to 25 minutes, the percentage of methanol was increased until the solvent was 100% methanol. The ratio was held at 100% methanol for the next 10 minutes. During the last 5 minutes, the solvent mixture was returned to the starting ratio of 75% methanol: 25% water (0.1% TFA).

Polarography

Polar band 2 was analyzed with the assistance of Dr. Ferren using an Epsilon Controlled Growth Mercury Electrode from Bioanalytical Systems. Two solvents with two different supporting electrolytes were used: 0.1 M TBAHFP (tetrabutylammonium

hexafluorophosphate, Fluka, 98.0% pure) in 100% methanol and 0.1 M NaCl in 33% deionized water: 66% methanol. The A2E from polar band 2 was added to each solution until color was visible. Two scans were performed on each A2E solution. Blanks containing only the supporting electrolytes (0.1 M TBAHFP or 0.1 M NaCl) were also run. All TBAHFP solutions were scanned from 0 to -800 mV after an initial scan from 0 to -1800 mV revealed that the current stopped increasing significantly by -800 mV. The solutions containing NaCl were scanned from 0 to -1800 mV. As recommended by Sawyer et al., (1984) nitrogen gas was bubbled through the polarographic cell prior to each run to remove dissolved oxygen. All scans were performed at a linear scan rate of 20 mV/s with a filter of 1.0 Hz and a quiet time of 2 seconds. Sample data was collected at 1 mV intervals.

The polarograms were used to calculate $E_{½}$ values and i_d values according to the method presented by Sawyer et al. (1984). The initial part of the curve, where the current increases gradually, is treated as the residual (baseline) current (Sawyer et al., 1984). A line is drawn tangent to this part of the curve to extend the residual current as shown in Figure 11 (Sawyer et al., 1984). The value of the limiting diffusion current (i_d) is determined by finding the distance between the residual current line and the maximum current of the reduction wave (Sawyer et al., 1984). The $E_{½}$ value is determined by drawing a line parallel to the residual current line that intersects the curve at ½ i_d; the x-value of this point of intersection corresponds to the potential known as $E_{½}$ (Sawyer et al., 1984).

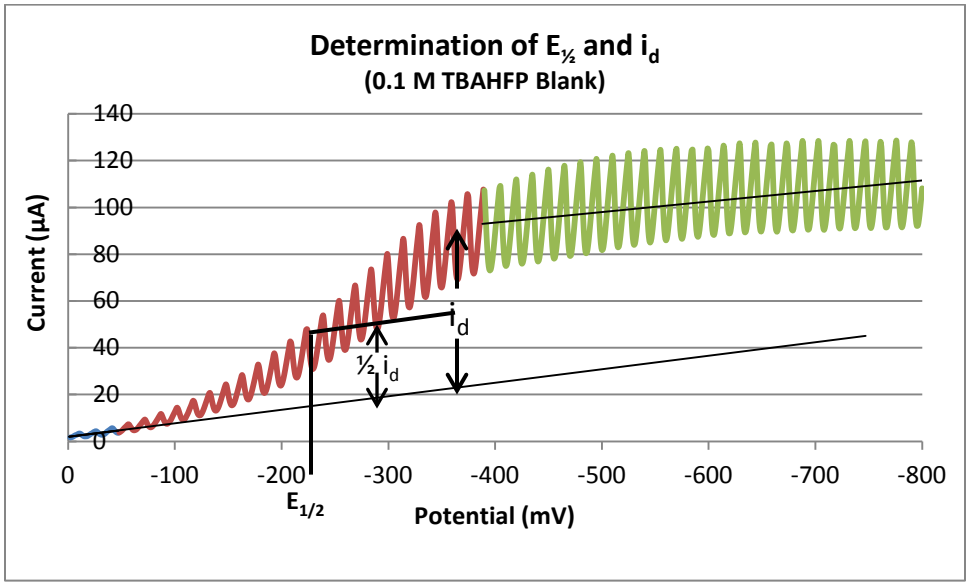

Figure 11. Sample polarogram showing the determination of $E_{½}$ and i_d.
The polarogram for the 0.1 M TBAHFP solution is used to demonstrate the calculation of $E_{½}$ and i_d. The initial baseline current is shown in blue; the reduction wave is shown in red, and the final current after the limiting diffusion current has been reached is shown in green.

RESULTS

HPLC Analysis

HPLC analysis of the band that was tested polarographically (polar band 2) indicated that the band contained A2E. The presence of A2E is indicated by the appearance of absorbance peaks at approximately 330 and 430 nm; the absorbance peak at 430 nm should be higher (Parish et al., 1998). During previous work with A2E in our laboratory, the absorption peaks of A2E appeared at a retention time (R_T) of approximately 20 minutes (Taylor et al., 2007; White et al., 2011). In the present study, the strongest absorption peaks at 330 and 430 nm occurred at 39 minutes, and, unlike previously reported results, the peak at 330 nm was higher than the peak at 430 nm (Fig. 12). This abnormality may indicate that the A2E sample contained impurities or that the HPLC column contained particulate impurities. However, the strong absorbance peaks at 330 and 430 nm indicated that A2E was likely present in polar band 2. A similar set of absorbance peaks was obtained when polar band 3 was analyzed by HPLC.

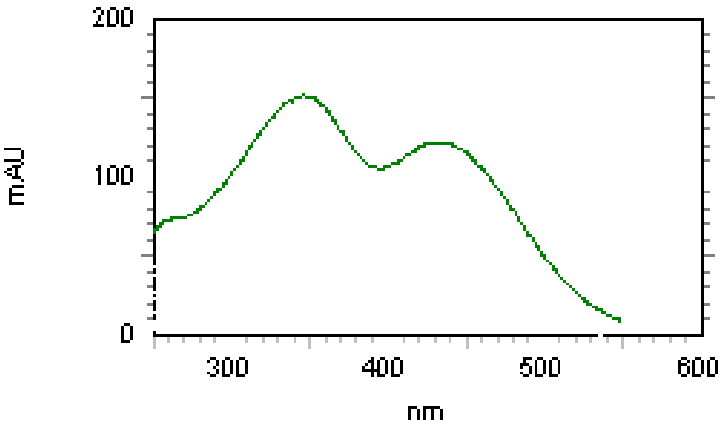

Figure 12. Absorbance spectrum for polar band 2 at 39.00 minutes.

Polarographic Analysis

Reduction waves occurred in each polarographic trial. Each reduction wave had the shape of a sigmoidal curve: the current increased sharply over an interval of approximately 200 mV, then leveled off. The polarograms for each of the six polarographic trials are shown in Figures 13-18. Tables 1 and 2 list the $E_{½}$ and i_d values calculated for each trial.

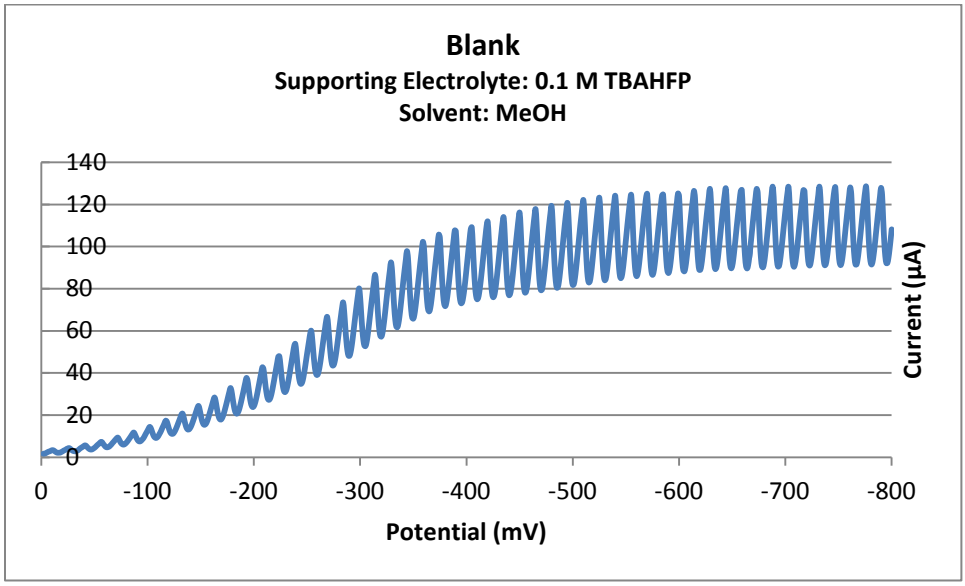

Figure 13. Polarogram for the TBAHFP blank solution (a methanol solution containing only TBAHFP).

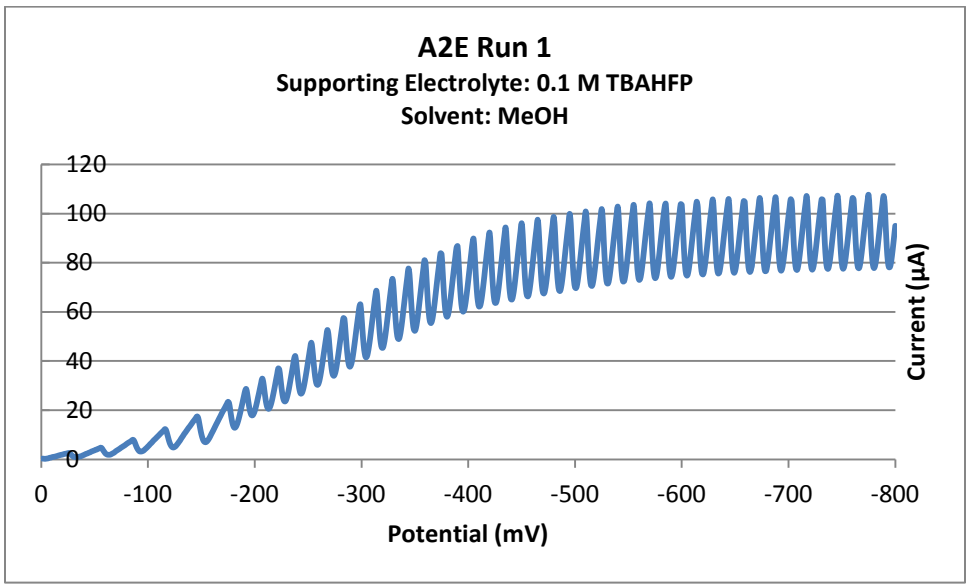

Figure 14. Polarogram for the first trial with an A2E solution containing TBAHFP as the supporting electrolyte.

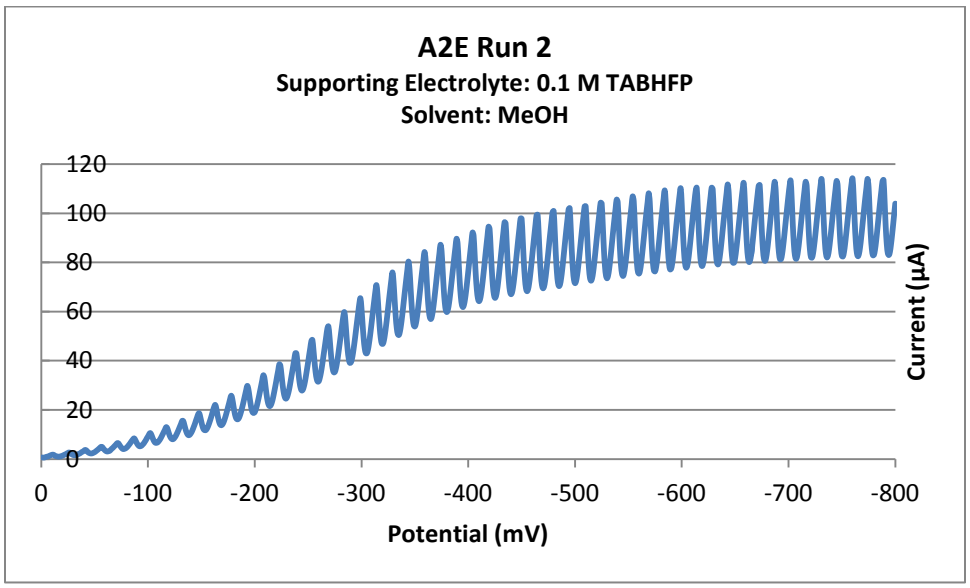

Figure 15. Polarogram for the second trial with an A2E solution containing TBAHFP as the supporting electrolyte.

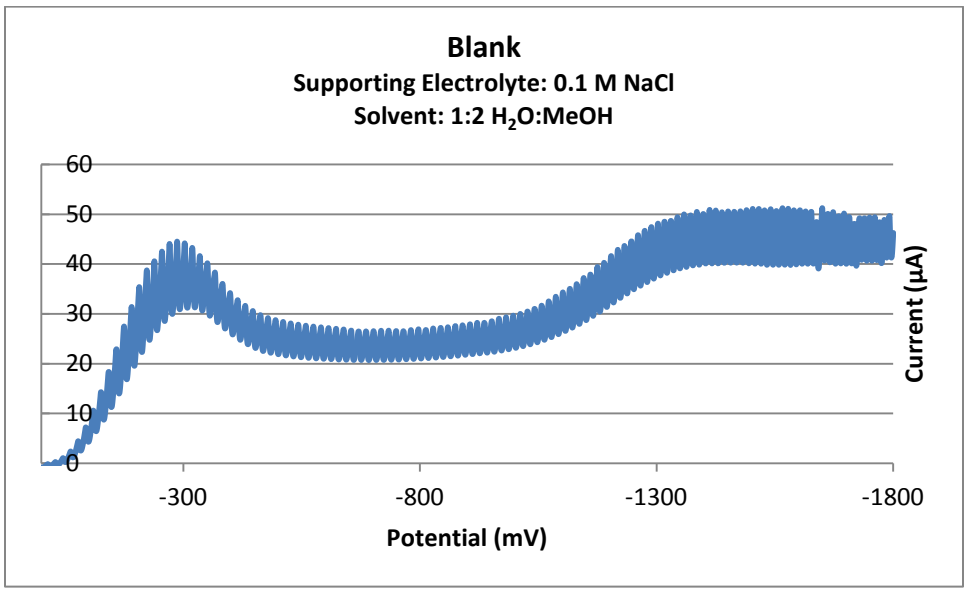

Figure 16. Polarogram for the NaCl blank solution (1:2 water:methanol solution containing only NaCl).

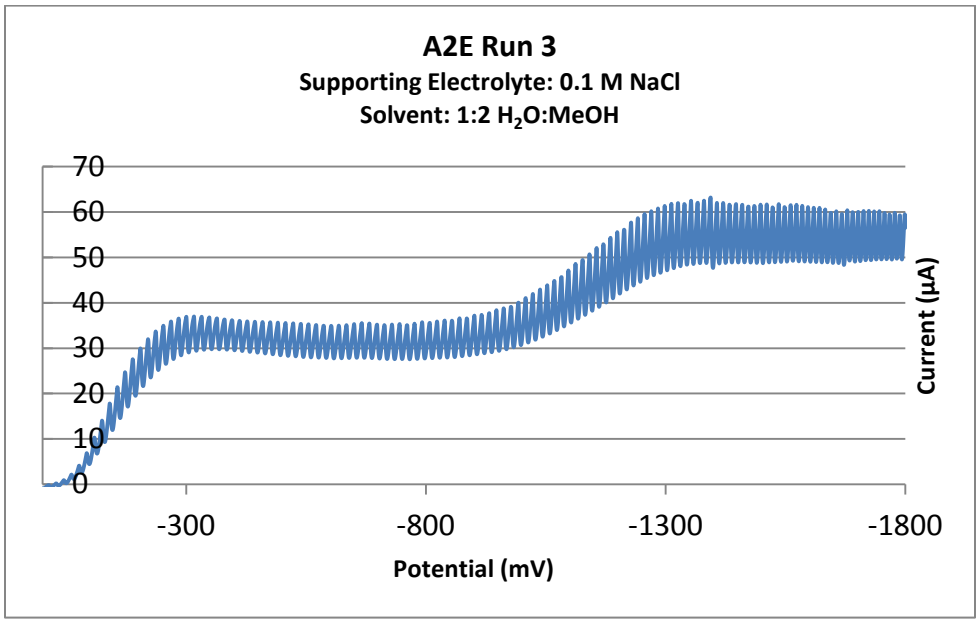

Figure 17. Polarogram for the first trial with an A2E solution containing NaCl as the supporting electrolyte.

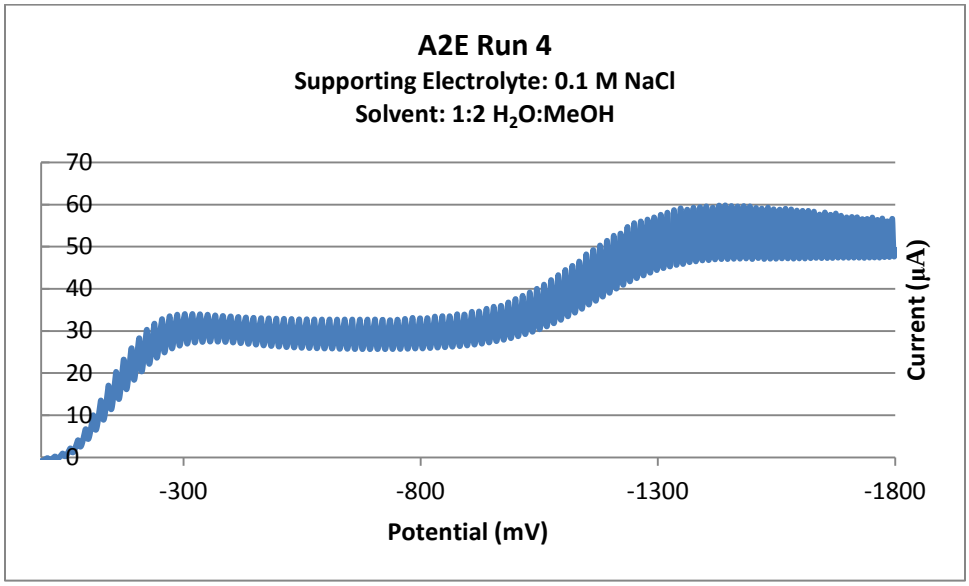

Figure 18. Polarogram for the second trial with an A2E solution containing NaCl as the supporting electrolyte.

Table 1. i_d and $E_{½}$ Values for TBAHFP Solutions

Sample Name	i_d (µA)	$E_{½}$ (mV)
Blank	115	-252
A2E Run 1	87	-250
A2E Run 2	92.5	-267

Table 2. i_d and $E_{½}$ Values for NaCl Solutions

Sample Name	Wave 1 i_d (µA)	Wave 2 i_d (µA)	Wave 1 $E_{½}$ (mV)	Wave 2 $E_{½}$ (mV)
Blank	37	28	-150	-1119
A2E Run 3	35	31	-141	-1128
A2E Run 4	43	23	-153	-1191

For both supporting electrolytes (0.1 M TBAHFP and 0.1 M NaCl), the A2E samples yielded polarograms with reduction waves very similar to those observed for the blank samples. More specifically, the polarograms of the blanks and corresponding A2E solutions had reduction waves with similar sizes, shapes, and placement along the x-axis.

The 0.1 M TBAHFP solutions (both the A2E samples and the blank; Fig. 13-15) each produced a single reduction wave. The $E_{½}$ values of these waves ranged from approximately -250 to -267 V. Graphically, the small range of $E_{½}$ values means that all three reduction waves begin at approximately the same potential along the x-axis (Sawyer et al., 1984). The three waves also have similar i_d values, meaning that all three waves have similar heights and reached similar maximum currents.

The 0.1 M NaCl solutions (both the blank and those with A2E; Fig. 16-18) produced polarograms with two reduction waves. Again, the narrow range of $E_{½}$ values indicates that the reduction waves in each trial may have resulted from the reduction of the same species. The $E_{½}$ values of the first waves ranged from -141 to -153 V; the $E_{½}$ values of the second waves ranged from -1120 to -1200 V. The heights of the waves were also quite similar from one trial to another: the i_d values of the first waves had a range of 8 μA; the i_d values of the second waves had a range of merely 3 μA.

DISCUSSION

Polarographic analysis of A2E from polar band 2 yielded polarograms that were practically identical to those of the corresponding blank solutions in regard to reduction wave number, shape, height (i_d) and position on the x-axis ($E_{½}$). Trials with the 0.1 M TBAHFP solution and the corresponding blank produced one-wave polarograms, while trials with 0.1 M NaCl solutions yielded polarograms with two waves. The similarities among the polarograms for all three trials with each solution suggest that the dropping mercury electrode may have been responding to the reduction of a species other than A2E.

Since the reduction waves produced were virtually the same whether or not A2E was present, it appears that another species present in the solution underwent reduction instead of A2E. It is possible that the solvent underwent reduction in all six trials. In that case, the difference between the reduction waves of the 0.1 M TBAHFP and 0.1 M NaCl solutions could be explained by the difference in solvent composition (100% methanol for TBAHFP and 2:1 methanol: water for NaCl). However, water is commonly used as a polarographic solvent, and methanol has been used in polarographic analyses of organic compounds successfully, although the best results were obtained with anhydrous methanol (Rogers and Kipnes, 1955). It therefore seems improbable that the reduction waves were caused by the solvent.

Another possibility is that TBAHFP (one of the supporting electrolytes) underwent reduction. Previously, TBAHFP was used as the supporting electrolyte during CV scans of A2E solutions (White et al., 2010). The results indicated that the

voltammeter could have been responding to the oxidation and reduction of TBAHFP instead of measuring the redox response of A2E. However, this hypothesis would not explain the reduction waves seen in NaCl solutions. It should also be noted that other researchers have reported successfully using TBAHFP as a supporting electrolyte during CV analysis of carotenoids (Jeevarajan et al., 1996).

It is more likely that the contaminating species was oxygen. The reduction of dissolved oxygen is known to produce large reduction waves (Sawyer et al., 1984). Perhaps nitrogen was not bubbled through the polarographic cell for a long enough period of time to remove all dissolved oxygen.

Regardless of which species caused the reduction response observed in the present study, it was clear from the response produced by the blank solutions that the reduction of A2E was not being measured reliably. The A2E concentration or level of purity may have been too low for a reduction wave from A2E to be observable. The abnormalities observed in the absorbance spectrum of our A2E sample support the idea that the A2E sample was not completely pure. It is also possible that the A2E concentration was so low that its reduction could not be detected voltammetrically. Or perhaps the reduction of A2E is not a straightforward, reversible redox reaction and therefore cannot be detected by simple CV or polarographic analysis.

CONCLUSIONS

In this study, A2E was analyzed polarographically with the goal of finding an estimate for its reduction potential. Because previous cyclic voltammetry trials yielded variable results, A2E was analyzed polarographically to eliminate the possibility of electrode contamination over time. However, the results of the present study indicate that there are other difficulties associated with studying A2E electrochemically. One such difficulty is the task of synthesizing and purifying an adequate amount of A2E. Separation by silica gel gravity column chromatography is time-consuming and does not afford highly pure samples. Separation by HPLC yields purer samples but is even more time-consuming and requires more solvent.

The reduction waves produced by the blank solutions present another obstacle, because they indicate that the polarograph was responding the reduction of something other than A2E. The first step in solving this problem could be simply bubbling nitrogen through each blank solution for a longer period of time (5-10 minutes) before performing polarography (El-Enany et al., 2009; Prasad and Rao, 2010). If the contaminating species is dissolved oxygen, this procedure may eliminate reduction responses in the blank solutions. If a baseline reading without a significant reduction wave can be obtained, further experiments can be performed to a find a supporting electrolyte and solvent combination suitable for dissolving A2E and allowing reduction waves to be measured.

Another experimental modification that could be tested in future studies would be to use a more concentrated sample of A2E. This could be accomplished by reducing

the amount of solvent used to prepare A2E solutions for polarography. Combining multiple A2E-containing fractions could also help increase its concentration. This may help correct for the possibility that there was not enough A2E present in the sample solutions to be detected. Another approach would be to separate A2E by cation exchange chromatography instead of silica gel chromatography (Jee et al., 2012). This method could be used to speed the preparation of A2E, decreasing the amount of time that A2E is exposed to light, which in turn would increase the purity of A2E by decreasing the rate of photoisomerization to other compounds.

In conclusion, it is not yet clear if measuring the reduction potential of A2E via polarography is a viable option. It is possible that polarography and other types of voltammetry are not effective methods for studying the reduction of A2E due to its unique characteristics, such as the positively-charged nitrogen of the pyridine ring. However, there are several procedural modifications that should be investigated before polarography is ruled out as a method for characterizing the reduction of A2E.

REFERENCES

Baehr, W.; Liebman, P. Visual cascade. In *Encyclopedia of Life Sciences*. Macmillan: London, 2002.

Baylor, D. How photons start vision. *Proc. Natl. Acad. Sci. USA.* **1996**, *93*, 560-565.

Ben-Shabbat, S.; Parsish, C. A.; Vollmer, H. R.; Yasuhiro, I.; Fishkin, N.; Nakanishi, K.; Sparrow, J. R. Biosynthetic studies of A2E, a major fluorophore of retinal pigment epithelial lipofuscin. *J. Biol. Chem.* **2002**, *277*, 7183-719.

Bioanalytical Systems, Inc. Polarographic analysis. http://www.basinc.com/services/pharm-polarographic.html (accessed Nov, 2012).

Birnbach, C. D.; Järveläinen, M.; Possin, D.E.; Milam, A. H. Histopathology and immunocytochemistry of the neurosensory retina in fundus flavimaculatus. *Ophthalmology* **1994**, *101,* 1211-1219.

Boulton, M.; Dontsov, A.; Jarvis-Evans, A.; Ostrovsky, M.; Svistunenko, D. Lipofuscin is a photoinducible free radical generator. *J. Photochem. Photobiol., B.* **1993**, *19*, 201-204.

Cideciyan, A. V.; Aleman, T. S.; Swider, M.; Schwartz, S. B.; Steinberg, J. D.; Brucker, A. J.; Maquire, A. M.; Bennet, J.; Stone, E. M.; Jacobson, S. G. Mutations in ABCA4 result in accumulation of lipofuscin before slowing of the retinoid cycle: A reappraisal of the human disease sequence. *Hum. Mol. Genet.* **2004**, *13*, 525-534.

Crouch, R. K.; Chader, G. J.; Wiggert, B.; Pepperburg, D. R. Invited review: Retinoids and the visual process. *Photochem. Photobiol.* **1996**, *64,* 613-621.

Cyberlipid Center: Ethanolamine glycerophospholipids. http://www.cyberlipid.org/phlip/pgly04.htm (accessed Mar 16, 2013).

Cyberlipid Center: Vitamin A. http://www.cyberlipid.org/vita/vita0003.htm (accessed Mar 16, 2013).

Dorey, C. K.; Wu, G.; Ebenstein, D.; Garsd A.; Weiter, J. J. Cell loss in the aging retina. *Invest. Ophthalmol. Visual Sci.* **1989**, *30,* 1691-1699.

Dowling, J. E. *The retina: An approachable part of the brain.* Belknap Press: Cambridge, MA, 1987.

Ebbing, D. D.; Gammon, S. D. *General Chemistry,* 9th ed.; Houghton Mifflin: Boston, 2009.

Einbock, W.; Moessner, A.; Schnurrbursch, U. E.; Holz, F. G.; Wolf, S. Changes in fundus autofluorescence in patients with age-related maculopathy. Correlation to visual function: A prospective study. *Graefe's Arch. Clin. Exp. Ophthalmol*. **2005**, *243,* 300-305.

Eldred, G. E.; Lasky, M. R. Retinal age pigments generated by self-assembling lysosomotropic detergents. *Nature* **1993**, *361*, 724-726.

El-Enany, N., El-Brashy, A.; Belal, F.; El-Bahay, N. Polarographic analysis of quetiapine in pharmaceuticals. *Port. Electrochim. Acta* **2009**, *27,* 113-125.

Feeney-Burns, L.; Hilderbrand E. S.; Eldridge, S. Aging human RPE: Morphometric analysis of macular, equatorial and peripheral cells. *Invest. Ophthalmol. Visual Sci.* **1984**, *25,* 195-200.

Fisiologiauhu: Anatomía del Sistema Visual. https://fisiologiavisualuhu.wikispaces.com/Anatom%C3%ADa+del+Sistema+Visual (accessed Mar 16, 2013).

Gaillard, E. R.; Atherton, S. J.; Eldred, G.; Dillon, J. Photophysical studies on human retinal lipofuscin. *Photochem. Photobiol.* **1995**, *61*, 448-453.

Hargrave, P. A. Rhodopsin structure, function, and topography: The Friedenwald lecture. *Invest. Ophthalmol. Visual Sci.* **2001**, *42*, 3-9.

Hargrave, P. A.; Hamm, H. E.; Hofmann, K. P. Interaction of rhodopsin with the G-protein, transducin. *BioEssays* **1993**, *15*, 43-50.

Hattar, S.; Liao, H.-W.; Takao, M.; Berson D. M.; Yau, K.-W. Melanopsin-containing retinal ganglion cells: Architecture, projections, and intrinsic photosensitivity. *Science* **2002**, *295,* 1065-1070.

Heo, G. Y.; Liao, W. L.; Turko, I. V.; Pikuleva, I. A. Features of the retinal environment which affect the activities and product profile of cholesterol-metabolizing cytochromes P450 CYP27A1 and CYP11A1. *Arch. Biochem. Biophys.* **2012**, *518*, 119-126.

Hogan, M. J. Role of the retinal pigment epithelium in macular disease. *Trans. - Am. Acad. Ophthalmol. Otolaryngol.* **1972**, *78*, 64-80.

Hofmann, K. P.; Pulvermuller, A.; Buczylko, J.; van Hooser, P.; Palczewski, K. The role of arrestin and retinoids in the regeneration pathway of rhodopsin. *J. Biol. Chem.* **1992,** *267*, 15701-12706.

Holz, F. G.; Bellman, C.; Staudt, S.; Schutt, F.; Volcker, H. E. Fundus autofluorescence and development of geographic atrophy in age-related macular degeneration. *Invest. Ophthalmol. Visual Sci.* **2001**, *42*, 1051-1056.

Ishiguro, S.; Suzuki, Y.; Tamai, M.; Mizuno, K. Purification of retinol dehydrogenase from bovine retinal rod outer segments. *J. Biol. Chem.* **1991**, *266,* 15520-15524.

Jager, F.; Palczewski, K.; Hofmann, K. P. Opsin/*all-trans*-Retinal complex activates transducin by different mechanisms than photolyzed rhodopsin. *Biochemistry* **1996**, *35,* 2901-2908.

Jager, F.; Jager, S.; Krautle O.; Friedman, N.; Sheves, M.; Hofmann, K. P.; Siebert, F. Interactions of the β-ionone ring with the protein in the visual pigment rhodopsin control the activation mechanism. An FTIR and fluorescence study on artificial vertebrate rhodopsins. *Biochemistry* **1994**, *88*, 7389-7397.

Jee, E. H.; Kim, S. R.; Jang, Y. P. Rapid purification method for vitamin A-derived aging pigments A2E and iso-A2E using cation exchange resin. *J. Chromatogr., A.* **2012**, *1251*, 232-235.

Jeevarajan, J. A.; Wei, C. C.; Kispert, L. D. Optical absorption spectra of dications of carotenoids. *J. Phys. Chem.* **1996**, *100,* 5637-5641.

Katz, M. L.; Gao, C. L.; Rice, L. M. Formation of lipofuscin-like fluorophores by reaction of retinal with photoreceptor outer segments and liposomes. *Mech. Ageing Dev.* **1996**, *92*, 159-174.

Kennedy, C. J; Rakoczy, P. E.; Constable, I. J. Lipofuscin of the retinal pigment epithelium: A review. *Eye* **1995**, *9*, 763-771.

Kolb, H. How the retina works. *Am. Sci.* **2003**, *91,* 28-35.

Kolb, H.; Famiglietti, E. V. Rod and cone pathways in the inner plexiform layer of the cat retina. *Science* **1974***, 186*, 47-49.

Kolb, H.; Nelson, R.; Ahnelt, P.; Cuenca, N. Cellular organization of the vertebrate retina. In *Concepts and Challenges in Retinal Biology: A Tribute to John E. Dowling;* Kolb, H., Ripps, H., Wu S., Eds.; Elsevier Press : Amsterdam, 2001; pp. 3-26.

Koryta, J. Theory of polarographic currents. *Electrochim. Acta* **1961**, *3*, 318-339.

Liu, J.; Itagaki, Y.; Ben-Shabbat, S.; Nakanishi, K.; Sparrow, J. R. The biosynthesis of A2E, a fluorophore of aging retina, involves the formation of the precursor, A2-PE, in the photoreceptor outer segment membrane. *J. Biol. Chem.* **2000***, 275*, 29354-29360.

Lopez P. F.; Maumenee I. H.; de la Cruz, Z.; Green, W. R. Autosomal-dominant fundus flavimaculatus: Clinicopathologic correlation. *Ophthalmology* **1990**, *97*, 798–809.

Parish, C. A.; Hashimoto, M.; Nakanishi, K.; Dillon, J.; Sparrow, J. R. Isolation and one-step preparation of A2E and *iso*-A2E, fluorophores from human retinal pigment epithelium. *Proc. Natl. Acad. Sci. U. S. A.* **1998**, *95*, 14609–14613.

Prasad, A. R.; Rao, V. S. Polarographic determination of certain cephalosporins in pharmaceutic preparations. *Res. Pharm. Sci*. **2010**, *5*, 57-63.

Pugh, E, N.; Lamb, T. D. Amplification and kinetics of the activation steps in phototransduction. *Biochim. Biophys. Acta* **1993**, *1141*, 111-149.

Radu, R. A.; Han, Y.; Bui, T. V.; Nusinowitz, S.; Bok, D.; Lichter, J.; Widder, K.; Travis, G. H.; Mata, N. L. Reductions in serum vitamin A arrest accumulation of toxic retinal

fluorophores: A potential therapy for treatment of lipofuscin-based retinal diseases*. Invest. Ophthalmol. Visual Sci.* **2005**, *46*, 4393-4401.

Ragauskaite, L.; Heckathorn, R. C.; Gaillard, E. R. Environmental effects on the photochemistry of A2-E, a component of human retinal lipofuscin. *Photochem. Photobiol.* **2001**, *74*, 483-488.

Randall, C. E.; Lewis, J. W.; Hug, S. J.; Bjorling, S. C.; Eisner-Shanas, I.; Friedman, N.; Kliger, D. S. A new photolysis intermediate in artificial and native visual pigments. *J. Am. Chem. Soc*. **1991**, *113*, 3473-3485.

Rando, R. R. Membrane phospholipids and the dark side of vision. *J. Bioenerg. Biomembr.* **1989**, *23*, 133-146.

Rando, R. R. Molecular mechanisms in visual pigment regeneration. *Photochem. Photobiol.* **1992**, 56, 1145-1156.

Reesk, J. F.; Farabakhsh, Z. T.; Hubbel, W. L.; Khorana, H. G. Formation of the meta II photointermediate is accompanied by conformational changes in the cytoplasmic surface of rhodopsin. *Biochemistry* **1993**, *32*, 12025-12035.

Ren, R. X. F.; Sakai, N.; Nakanishi, K. Total synthesis of the ocular age pigment A2E: A convergent pathway. *J. Am. Chem. Soc.* **1997**, *119*, 3619-3620.

Rodieck, R. W. *The First Steps in Seeing*. Sinauer Associates : Sunderland, MA, 1998.

Rogers, W.; Kipnes, S. M. Polarography of carbonyl compounds in methanol. *Anal. Chem.* **1955**, *27,* 1916–1918.

Rozanowska, M.; Wessels, J.; Boulton, M.; Burke, J. M.; Rodgers, M. A. J.; Truscott, T. G.; Sarna, T. Blue light-induced singlet oxygen generation by retinal lipofuscin in nonpolar media. *Free Radical Biol. Med.* **1998***, 24*, 1107-1112.

Saari, J. C. Retinoids in photosensitive systems. In *The Retinoids: Biology, Chemistry, and Medicine;* Sporn, M. B., Roberts, A. B., Goodman, D. S., Eds.; Raven Press: New York, 1994; pp. 351-379.

Saari, J. C.; Bredberg, L.; Noy, N. Control of substrate flow at a branch point in the visual cycle. *Biochemistry* **1994**, *33*, 3106-3112.

Sakai, N.; Decatur, J.; Nakanishi, K.; Eldred, G. E. Ocular pigment "A2-E": An unprecedented pyridinium bisretinoid. *J. Am. Chem. Soc.* **1996**, *118*, 1559-1560.

Sakmar, T. P.; Franke, R. R.; Khorana, H. G. Glutamic acid 113 serves as the retinylidene Schiff base counterion in bovine rhodopsin. *Proc. Natl. Acad. Sci. U. S. A.* **1989**, *86*, 8309-8313.

Sarks, S. H.; Van Driel, D.; Maxwell, L.; Killingsworth, M. Softening of drusen and subretinal neovascularization. *Trans. Ophthalmol. Soc. U. K.* **1980**, *100*, 414-422.

Sawyer, D. T.; Heineman, W. R.; Beebe, J. M. *Chemistry experiments for instrumental methods.* Wiley: New York, 1984.

Schmitz-Valckenberg S.; Bultmann, S.; Dreyhaupt, J.; Bindewald, A.; Holz, F. G.; Rohrschneider, K. Fundus autofluorescence and fundus perimetery in the junctional zone of geographic atrophy in patients with age-related macular degeneration. *Invest. Ophthalmol. Visual Sci*. **2004**, *45*, 4470-4476.

Skoog, D. A.; Holler, F. J.; Crouch, S. R. *Instrumental analysis* (India ed.). Cengage Learning: Delhi, India, 2007.

Spaide, R. F. Fundus autofluorescence and age-related macular degeneration. *Ophthalmology* **2003**, *110,* 392-399.

Sparrow, J. R.; Nakanishi, K.; Parish, C. A. The lipofuscin fluorophore A2E mediates blue light-induced damage to retinal pigmented epithelial cells. *Invest. Ophthalmol. Visual Sci*. **2000**, *41,* 1981-1989.

Sparrow, J. R.; Parish, C. A.; Hashimoto, M.; Nakanishi, K. A2E, a lipofuscin fluorophore, in human retinal pigmented epithelial cells in culture. *Invest. Ophthalmol. Visual Sci.* **1999**, *40*, 2988-2995.

Sparrow, J. R.; Vollmer-Snarr, H. R.; Zhou, J.; Jang, Y. P.; Jockusch, S.; Itagaki, Y.; Nakanishi, K. A2E-epoxides damage DNA in retinal pigment epithelial cells. *J. Biol. Chem.* **2003**, *278*, 18207-18213.

Sparrow, J. R.; Zhou, J.; Ben-Shabbat, S.; Vollmer, H.; Itagaki, Y.; Nakanishi, K. Involvement of oxidative mechanisms in blue-light-induced damage to A2E-laden RPE. *Invest. Ophthalmol. Visual Sci.* **2002**, *43*, 1222-1227.

Suzuki, Y.; Ishiguru, S.; Tamai, M. Identification and immunohistochemistry of retinol dehydrogenase from bovine pigment epithelium. *Biochim. Biophys. Acta* **1993**, *1163*, 9794-9799.

Taylor, D.; Ferren, L.; Harper, W. *Studies with A2E and AGEs*. Pence-Boyce research at Olivet Nazarene University, Bourbonnais, IL, 2008.

Unger, V. M.; Hargrave, P. A.; Baldwin, J. M.; Schertler G. F. X. Arrangement of rhodopsin transducin membrane alpha-helices. *Nature* **1997**, *389*, 203-206.

Wald, G. The molecular basis of visual excitation. *Nature* **1968**, *219*, 800-807.

Wassel, J.; Davies, S.; Baedsley, W.; Boulton, M. The photoreactivity of the retinal age pigment lipofuscin. *J. Biol. Chem.* **1999***, 274*, 23,828-832.

White, E.; Ferren, L.; Harper, W. *Synthesis and cyclic voltammetry of A2E*. Poster session presented at Olivet Nazarene University, Bourbonnais, IL, 2010.

Yau, K.-W. Phototransduction mechanism in retinal rods and cones. *Invest. Ophthalmol. Visual Sci.* **1994**, *35*, 9-32.

Zhou, J.; Jang, Y. P.; Kim, S. R.; Sparrow, J. R. Complement activation by photooxidation products of A2E, a lipofuscin constituent of the retinal pigment epithelium. *Proc. Natl. Acad. Sci. U. S. A.* **2006**, *103*, 16182-16187.

Zhukovsky, E. A.; Oprian, D. D. Effect of carboxylic acid side chains on the absorption maximum of visual pigments. *Science* **1989**, *246*, 928-930.

Zimmerman, W. F. The distributions and proportions of vitamin A compounds during the visual cycle in the rat. *Vision Res.* **1974**, *14*, 795-802.

Zuman, P. Principles of applications of polarography and voltammetry in the analysis of drugs. *FABAD J. Pharm. Sci*. **2006**, *31,* 97-115.

APPENDIX 1: ABBREVIATIONS

A2E	N-retinylidene-N-retinylethanolamine (2 molecules of vitamin A aldehyde and one molecule of ethanolamine; Liu et al., 2000)
A2-PE	Phosphatidylethanolamine-bisretinoid (2 molecules of vitamin A derivatives and one molecule of phospatidylethanolamine; Liu et al. 2000)
AMD	Age-related macular degeneration
CV	Cyclic voltammetry
DME	Dropping mercury electrode
$E_{½}$	Potential corresponding to ½ i_d (Sawyer et al., 1984)
i_d	Limiting diffusion current (Sawyer et al., 1984)
HPLC	High-performance liquid chromatography
MeOH	Methanol
NaCl	Sodium chloride
RPE	Retinal pigment epithelium
R_T	Retention time
TBAHFP	Tetrabutylammonium hexafluorophosphate
TFA	Trifluoroacetic acid
UV	Ultraviolet